Sewing up the Wounds: A Robotic Suturing System for Flexible Endoscopy

Lin Cao*[,a]; Xiaoguo Li[a]; Phuoc Thien Phan[a]; Anthony Meng Huat Tiong[a]; Hung Leng Kaan[b]; Jiajun Liu[a]; Wenjie Lai[a]; Yanpei Huang[a]; Huu Minh Le[a]; Muneaki Miyasaka[a]; Khek Yu Ho[c]; Philip Wai Yan Chiu[d]; Soo Jay Phee[a]

ABSTRACT

If a perforation occurs as a result of a flexible endoscopic procedure, suturing through urgent laparoscopy or open surgery may be required to repair the perforation because suturing is normally stronger than closure using existing endoscopic devices. Suturing with stitches and knots, widely adopted in open or laparoscopic surgery, is still not possible in flexible endoscopy. This is because of the confined space of the natural orifice and target area, high levels of motion dexterity and force needed for stitching and knot-tying, and critical size and strength requirements of wound closure. We present a novel flexible endoscopic robotic suturing system that is able to suture gastrointestinal defects without opening up the patient's body like in open or laparoscopic surgery. This system features a robotic needle driver and a robotic grasper, both of which are flexible, through-the-scope (small in sizes), and dexterous with five degrees of freedom. The needle driver, facilitated by the grasper, enables the surgeon to control a needle through teleoperation to make stitches and knots in flexible endoscopy. Successful in vivo trials were conducted in the rectum of a live pig to confirm the feasibility of endoscopic suturing and knot-tying using the system in a realistic surgical scenario (not possible with existing devices which are all manually driven). This new technology will change the way how surgeons close gastrointestinal defects.

I. INTRODUCTION

A. *Clinical Needs*

Flexible endoscopy has drastically extended its reach from pure diagnosis to effective therapeutic treatments in the gastrointestinal tract over the years. However, these therapeutic treatments may result in significantly increased risks of perforations [1] with high death rates, e.g., the death rate of iatrogenic colonic perforations is as high as 5-25% [2, 3]. Secure closure of perforations is paramount to avoid leakage of gastrointestinal fluids into the abdomen which often leads to severe complications.

As flexible endoscopy plays an increasingly important role in therapeutic procedures, there is a rising demand for a reliable and effective endoscopic closure device in various procedures, from the widespread Endoscopic Submucosal Dissection (ESD), to Endoscopic Full-Thickness Resection (EFTR), and to Natural Orifice Transluminal Endoscopic Surgery (NOTES) [1]–a promising paradigm shift for minimally invasive abdominal surgery. ESD is an advanced endoscopic procedure to remove superficial gastrointestinal mucosa tumors through en-bloc resection. Requiring highly skillful operation, ESD has a high risk (up to 5-10% [1]) of perforations due to limited dexterity of tools and the lack of experience of the specialist. EFTR is an even more powerful procedure that removes tumors deep in the gastrointestinal muscular layer by resecting the full depth of the wall of the organ, which, however, results in a perforation requiring secure closure. NOTES is an emerging endoscopic approach which obtains access to the abdominal cavity through natural orifices (mouth, anus, vagina, etc.) and subsequently through an internal incision in the stomach, colon, or bladder. Although no incision is made on the skin, an internal full-thickness perforation on the hollow organ is purposely created for NOTES internal access. All these procedures require effective endoscopic defect closure devices. In fact, despite the high potential as a paradigm shift, NOTES is still not widely adopted in clinical practice, and one of the main reasons is the lack of tools for reliable, surgical-quality closure of defects [4].

B. *Flexible Endoscopic Defect Closure Devices*

Hemoclips, normally used to stop gastrointestinal bleeding, are sometimes used for defect closure [5], but they are suitable only for shallow and small defects at the mucosal layer due to small closing force and opening range. Therefore, both industry and academia have made extensive research efforts to develop stronger and dedicated devices for defect closure in flexible endoscopy. Two devices are commercially available, i.e., the Over-The-Scope Clip (OTSC, Ovesco Endoscopy Inc., Germany) [6] and OverStitich (Apollo Endosurgery Inc., US) [7]. OTSC is a large superelastic nitinol flexure clip mounted on the tip of the endoscope. Once released, OTSC can efficiently clip the defect (suctioned to the clipping area) with approximately 8-9 N force. If more clips or other tools are needed, the endoscope needs to be withdrawn for reloads or tool exchanges during the procedure. Furthermore, injuries to surrounding organs may occur due to suction, and the clip's position cannot be adjusted when misfired. OverStitch is the only device that can make running stitches for flexible endoscopy. Again, it must be mounted on the tip of the endoscope due to its large size, which requires endoscope withdrawal for tool exchanges. In addition, tying standard surgical knots is still not possible with OverStitch and thus a fastening element is employed to secure the stitches. Some other prototypes for endoscopic defect closure have also been developed, but they all have individual intrinsic problems that limit their clinical potentials [8].

Thus far, suturing with stitches and knots, the widely used traditional approach in open or laparoscopic surgery, is still not possible for flexible endoscopy. This unmet need might be because of the confined and unstructured space of the orifice and target area, high levels of motion dexterity and force needed for suturing and knot tying, and critical size and strength requirements of wound closure. Emerging novel technologies, especially the evolving robotic platforms for flexible endoscopy [9] and the widespread da Vinci system, have fired up our imagination of using robotics technologies to overcome the challenges faced by endoscopic suturing. Robotics may benefit the suturing task with enhanced dexterity, larger forces, reduced tool size, and more intuitive control, leading to surgical-quality closure. Meanwhile, although many flexible endoscopic robotic systems [9] have been developed in the past decade, they are

[a] School of Mechanical and Aerospace Engineering, Nanyang Technological University, Singapore.
[b] Department of Surgery, National University Hospital, Singapore.
[c] Yong Loo Lin School of Medicine, National University of Singapore, Singapore.
[d] Department of Surgery, Chinese University of Hong Kong, Hong Kong.
*Correspondence to lin.cao@ntu.edu.sg.

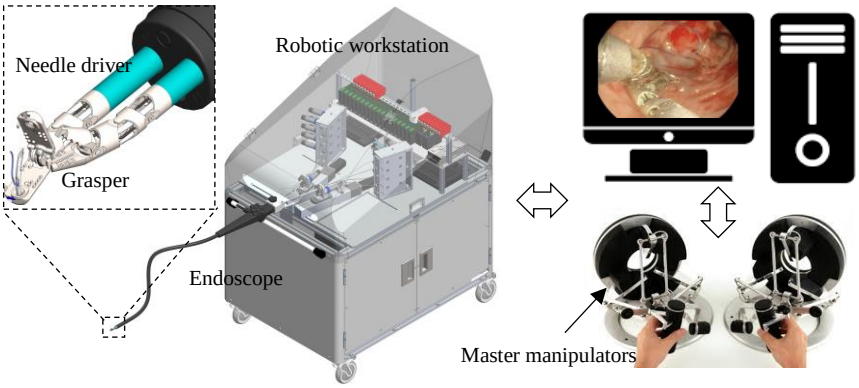

Figure 1. The flexible endoscopic robotic suturing system

all for diagnosis or the removal of diseased tissue by cutting while the more complicated task—repairing the resulted wounds via suturing—are not possible with these systems.

Here, we present a robotic suturing system that can desirably close wounds in flexible endoscopy with stitches and knots. The system features two flexible robotic arms—a dedicated needle driver[1] and a grasper. The needle driver enables the surgeon to robotically manipulate a curved, double-point needle to penetrate tissue at desired locations and angles. A latching mechanism is employed to switch the needle between the two jaws of the needle driver, which is crucial to generate stitches and knots. The grasper assists the needle driver by manipulating tissues and the suture thread. The advantageous features of the system are as follows:

(1) Flexible: the instruments are driven by flexible tendon sheath mechanisms (TSMs), suitable for the tortuous gastrointestinal (GI) tract.
(2) Dexterous: both instruments have five degrees of freedom (DOFs), which is vital for tissue and suture manipulation in confined areas.
(3) Through-the-Scope: the instruments are small enough to be inserted through the endoscope's tool channels, avoiding the withdrawal and re-insertion of the endoscope for tool exchanges or needle reloading.
(4) Running stitches: stitches can be continuously created for efficient and reliable closure.
(5) Knot-tying: knots can be tied for secure closure.
(6) Controlled/safe puncture: the surgeon can see the target tissue and needle tips, avoiding inadvertently injuries to surrounding organs [4].
(7) Full-thickness: full-thickness closure is possible with the system, promoting strong and reliable closures of life-threading perforations [4].
(8) Intuitive dual-arm operation: suturing is normally done with two arms, which is now achieved by the two cooperative robotic instruments and the intuitive mapping between the master and slave manipulators.

A part of this work was published in [10], this article additionally presents (1) an in vivo animal study of the system to confirm the feasibility of the concept in realistic surgical scenarios, (2) systematic force measurements of the penetrating process on biological colon and stomach tissues of different thicknesses, (3) systematic measurements of the force capacities of the instruments with the joints at different angles, (4) control with haptic force feedback, and (5) an in-out-out-in suturing pattern and the comparison of different ways of puncturing tissue based on both clinical practices and the features of these two new instruments.

Note that a suturing device for laparoscopy, Endo Stitch (Medtronic, USA), also employs a similar concept of passing a needle between two jaws for suturing. However, Endo Stitch is a rigid and large manual tool (Ø10 mm) only for laparoscopy. The proposed needle driver is much smaller (Ø4.4 mm), dexterous (5-DOF), flexible (driven by flexible TSMs) and robotically-driven. These unique features make the device particularly suitable for flexible endoscopy.

II. Design and Implementation

A. *System Overview*

With the system, the surgeon at the master console controls two slave robotic instruments (inside the flexible endoscope) via a robotic workstation (Figure 1). Two Omega 7 interfaces (Force Dimension Inc., Switzerland) are used as the master manipulators. The workstation consists of the motor blocks, control boards, and a docking adaptor for the endoscope. The endoscope[2] has two tool channels where the two robotic instruments—the needle driver (Ø4.4 mm) and grasper (Ø4.2 mm)—can be smoothly inserted. There is another standard channel for Ø2.5 mm manual endoscopic tools (needle injectors, Dual Knife, etc.). Details of the motor blocks are provided in Supplementary Material A.

B. *Needle Driver and Grasper*

The needle driver (Figure 2) has a pitch-yaw wrist and an end-effector manipulating a hollow, curved needle (gauge 21) with two lancet tips. The needle stands in-between the two jaws of the needle driver. A latching mechanism is employed to selectively lock the needle to one of the two jaws (Figure 2b and c). Each jaw has a locking blade that is driven by a TSM to lock or unlock the needle. The blades are attached to a tendon which is looped around three pulleys on the needle driver (Figure 2c). The blades are made by securely crimping a stainless tube (Length 5.5 mm, OD/ID: 1.07mm/0.84mm) flat onto the driving tendon, avoiding the delicate and complex laser welding procedure as previously described in [10]. When the tendon is pulled at one end, the corresponding blade will be advanced to engage with the needle, and the other blade is moved back to disengage, i.e., the needle is locked to one jaw and released on the other during suturing.

[1] A PCT patent on this needle driver has been filed (PCT/SG2018/050606).

[2] This endoscope is customized by EndoMaster Pte. Ltd., Singapore. No detailed information is permitted to be disclosed in this publication.

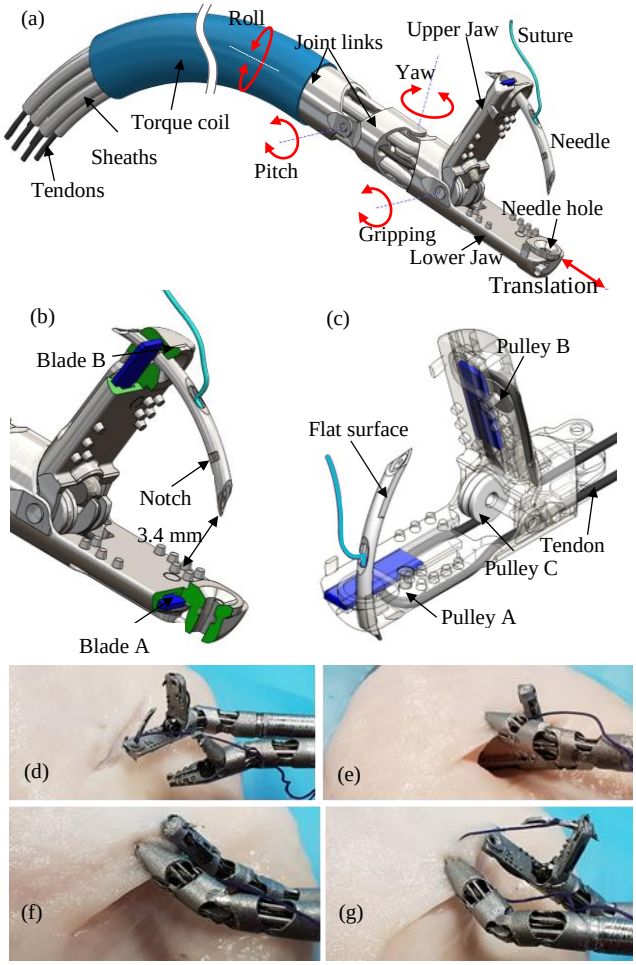

Figure 2. Needle driver: (a) overview; (b)-(c) switching needle between two jaws; (d)-(g) stitching process.

The needle has a flat region on each end [10] to constrain the needle from rotating inside the needle hole and to define the insertion depth of the needle. This ensures that the needle can always point to the needle hole on the opposite jaw and the blade can accurately slide into the corresponding slot. Note that the needle and needle holes are curved with a radius the same as that (9 mm) of the needle's motion trajectory (rotation around the gripping axis) to reduce friction and tissue trauma.

Both instruments have five DOFs (Figure 2a): gripping, yaw, pitch, roll, and translation. Thus, they can reach target tissues with suitable orientations (without steering the endoscope) and triangulate with each other. The grasper can precisely reach the target tissue and feed it to the needle tip, preventing blind puncture to surrounding organs [8]. The roll and translation DOFs of the instruments are achieved by rolling and translating the whole bodies of the instruments using motorized linear slides and gears on the motor blocks. The main body (torque coil) of each instrument is flexible in bending but stiff in transmitting torques in the tortuous endoscope. A problem with the previous prototype in [10] is that the torque coil has large elongation which introduces motion backlash for the translation DOF. In the current prototype, this backlash issue is solved by constraining the length of the torque coil using an inner tendon which is fixed to the two ends of the torque. In addition, when the endoscope is highly tortuous and there are large external loads on the end-effector, critical torsional backlash and uncontrollable torsional snapping may still occur, which is a safety concern. Therefore, the instruments can only be rolled to adjust the orientation only when there is no external load on the end-effector.

The dimensions, materials, and fabrication methods of the components can be found in [10]. The dimensions were selected with the following constraints: (1) the rigid sections of the instruments should be reasonable short to ensure smooth insertion of the instruments into the endoscope even when the endoscope is bend with 65 mm bending radius; (2) the instruments should at least have a cylindrical workspace of Ø25 mm; (3) the needle driver should be able to open wide and to exert enough forces to puncture tissue that are 3 mm in thickness [11] for full-thickness suturing; (4) the needle should be inserted into the jaws sufficiently deep to ensure stability, and the lancet tip of the needle should be sharp. The ranges of motion of the master manipulators and the robotic instruments are given in Table 1. The rolling range of the instruments is not limited.

Table 1 Motion ranges of the robotic arms.

	Slave	Master
Gripping	[0, 78]˚	[0, 28]˚
Left/right	[-83, 83]˚	[-80, 80] mm
Up/down	[-83, 83]˚	[-40, 80] mm
Translation	[0, 90] mm	[0, 110] mm

C. *Suturing: stitching and knot-tying*

Suturing consists of two sub-tasks: creating stitches and tying knots. Figure 2d-g demonstrate a stitching process using the prototype. To align with clinical practices, proper stitching patterns should be followed. An example is illustrated in Figure 3a where the two defect edges on a colon are closed via two stitches. A stitch is first made by puncturing the wound edge on the left from the inner surface of the colon to the outer surface (Figure 3a.2), i.e., "in-out"; then, the second stitch is made by puncturing the tissue from the outer surface to the inner surface of the opposite edge (Figure 3a.3), i.e., "out-in". The overall pattern is "in-out-out-in pattern". Repeating this pattern generates running stitches. This pattern ensures that there is no suture segment between the two edges of the wound when they are pulled together and thus secures direct contact between the wound edges for optimal healing. Doing so also leaves both ends of the suture inside the lumen of the colon, facilitating subsequent knot-tying.

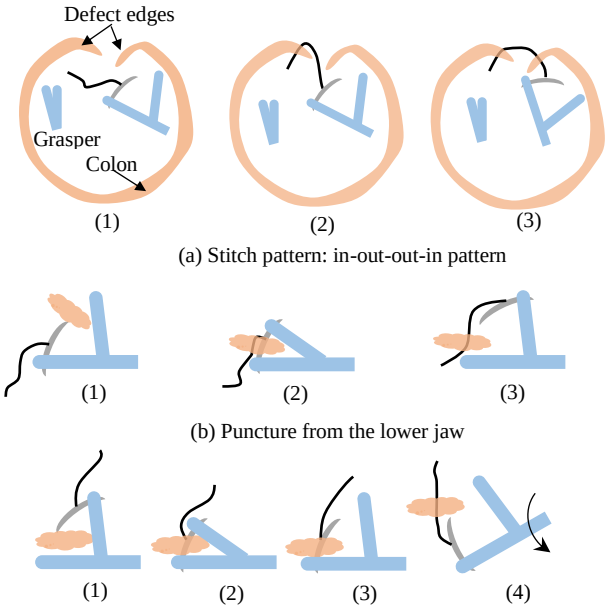

(a) Stitch pattern: in-out-out-in pattern

(b) Puncture from the lower jaw

(c) Puncture from the upper jaw

Figure 3. Stitching techniques

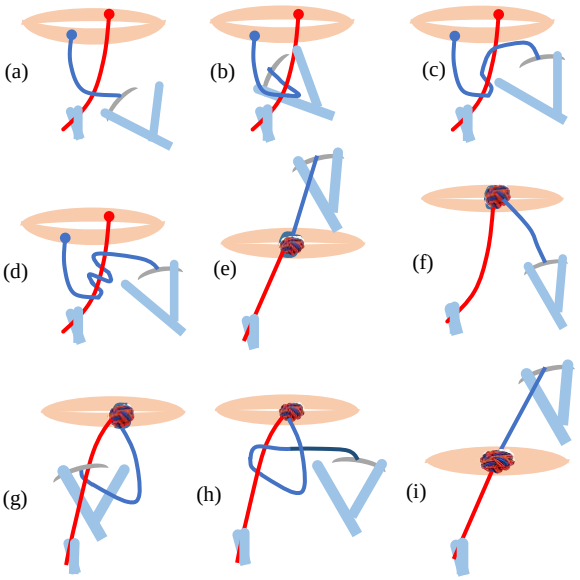

Figure 4. Tying a Surgeon's Knot using the two robotic arms

The tissue may be punctured with the needle initially either on the lower or upper jaw (Figure 3b and 3c). In Figure 3b, the needle is initially on the lower jaw. After puncturing the tissue, the needle is subsequently switched to the upper jaw. Opening the two jaws will conveniently pull the needle and suture through the tissue. In Figure 3c, the needle is initially on the upper jaw. After swapping the needle to the lower jaw, the whole end-effector has to be steered down to pull the needle and suture through the tissue (Figure 3c.4). This can be troublesome and inefficient because the colon wall (not shown here) below the end-effector would block this movement.

Tying knots is a traditional and widely adopted approach to securing stitches in surgery. The two basic procedures of knot tying are (1) creating a suture loop and (2) letting the needle pass through the loop. Figure 4 shows the schematic process of tying a Surgeon's Knot (with three simple overhand knots) using the two robotic arms. Thanks to the dedicate needle switching mechanism, passing the needle through the loop is simple and efficient. The knots can be tied by dragging the two ends of the suture with the two instruments in opposite directions.

D. *Needle deployment*

With the needle standing between the two jaws, the needle driver cannot be inserted through the tool channel because of a too large overall profile. To overcome this issue, A deployment mechanism using a super-elastic nitinol guidewire (Ø0.12 mm) is developed to deploy the needle so that the suturing device can still be delivered through-the-scope [10].

Once suturing is done, the needle can then be unlocked and subsequently unplugged from the needle hole using the grasper. Then, the grasper grips the needle so that it lies in-between its two jaws without exceeding the grasper's radial profile. The grasper, tightly gripping the needle, is then withdrawn through the tool channel. Finally, the needle driver can be withdrawn. If additional stitches are needed, the needle driver can be reloaded with a new needle and deployment guidewire.

III. Control Architecture

Each master manipulator provides a Ø160×110mm cylindrical workspace. The translational workspace is linearly mapped to that of the end-effector as listed in Table 1. The input (with a sampling rate of 1000 Hz) from Omega.7 devices is used as the PID control reference for the two motors associated with each DOF. When one motor winds in, its counterpart unwinds. Similarly, for the gripping motion, the [1, 28]˚ master motion range is linearly mapped to the [0, 78]˚ slave motion range. Moreover, once the master graspers reach [0, 1]˚, the puncturing and grasping programs are triggered for the slave suturing device and grasper correspondingly. The needle driver will keep driving the needle through the tissue until a maximum force of 90N is reached at the proximal end; then all movement on this TSM stops. Likewise, the slave grasper also delivers 90N on the pulling tendon and will keep holding this tension until the master grasper commands to release. This ensures that even if the tissue starts to slip from the grasper, the associated tendon would timely pull more to avoid further slipping.

For the two blades that switch the needle between upper and lower jaws, the switching process is triggered using the two add-on buttons on the right-hand Omega 7 device. When the upper button is pressed, the corresponding tendon will pull the upper blade until the proximal force reaches 30 N to ensure the blade is securely in position to lock the needle onto the upper jaw. Subsequently, the pulling motor will unwind 30˚ to release the tension (the blade still locks the needle) which, would otherwise, inhibits the movement of other joints. The same protocol applies to the lower blade.

The load cells provide valuable information for the control architecture. During the initialization protocol, both end-effectors stay inside their channels of the endoscope, and all motors wind in until 8N is reached for the closing-jaw tendons and 4N for all other tendons. This procedure ensures the yaw and pitch joints are in the neutral position and the jaws are fully closed. When manipulating the instruments in time of surgical procedures, load cells monitor the tension in all tendons to make sure no proximal force exceeds 100N so that we do not risk severe abrasion, breaking the tendon or buckling the sheath. The proximal tension is also used as force feedback for the pitch and yaw DOFs so that the user has a sense of the forces exerted on the tendons, avoiding excessive tissue manipulation force or tendon breakage. This scheme also allows the user to feel the hands' positions in the master workspace, which improves hand-eye coordination. For the gripping motion, without a resistive force to the thumb, the user can sometimes unintentionally trigger the automated grasping or puncturing process. Thus, for each Omega 7 interface, a small resistive force is applied to the user's thumb when the master gripper is in the range of [1, 3]˚ to eliminate false maneuvers.

IV. Benchtop Tests and In vivo Animal Trials

A. *Force capabilities of robotic instruments*

The output force capabilities of the two instruments were measured. To realistically include friction of TSMs in this measurement, the flexible body of each instrument was looped one round, i.e., with 360˚ of accumulative bending angle. The corresponding tendon was driven until its proximal load cell reaches around 90 N while the opposing tendon was released with the same displacement and other tendons kept the pretension (4N). The 90-N limit was to ensure the durability of the tendons. A load cell is connected to the tip of the instrument via a tendon to measure the output forces (Figure 5).

The gripping force is affected by the angles of the pitch and yaw joints because these angles increase the

accumulative angles of TSMs. Therefore, for gripping force measurement, each arm was measured at three different representative configurations which are defined by [pitch rotation, yaw rotation]: [0, 0]˚, [0, 83]˚ and [83, 83]˚ denoted as C1, C2, and C3, respectively.

The steering force of the yaw joint is affected by the angle of the pitch joint only, so two pitch rotations were considered for yaw steering force tests: 0˚ and 83˚denoted as C4 and C5, respectively.

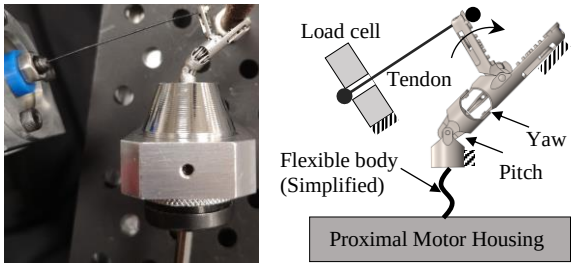

Figure 5. Setup for the gripping force measurement when the pitch joint is rotated: (a) physical setup, (b) schematic diagram. The setup was adjusted accordingly for C1~C6.

The steering force of the pitch joint is the most proximal joint and not affected by any other joints. Thus, the pitch steering force was measured by orienting the arm straight, denoted as C6.

Each configuration was measured five times. In-between these five-time measurements, the flexible body of the instrument was uncoiled and re-positioned.

B. *Puncture forces for ex vivo tissues*

Tests have also been done to measure the required force to puncture ex-vivo pig colon and stomach tissues using the needle. A motor drove the pulley of the needle driver (the lower jaw was fixed) through a linear bearing connected with tendons. A hollow load cell mounted on the bearing measured the force on the tendon (Figure 6) which was then converted to the gripping force on the needle using the mechanical advantage ratio of the upper jaw. The ratio was measured to be 6.05, which theoretically is 6 based on the moment arms of the upper jaw. Freshly packaged pig colon tissues and stomach tissues were purchased from a local supermarket. Tissues with different thicknesses were used: 1 mm, 2 mm, 3 mm for the colon; 2 mm, 3 mm, and 4 mm for the stomach. Each thickness category has five tissues, and each tissue was punctured once. Note that, due to the super flexible nature of the tissue, the thickness was roughly estimated without compressing the tissue.

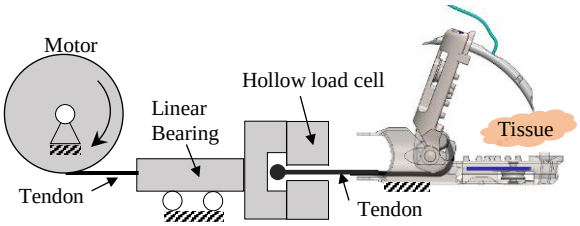

Figure 6. Schematic diagram of the setup for tissue puncture force measurement.

C. *In vivo animal trials*

This system was tested via a pilot in vivo animal study on a live pig (about 70 kg) with approval from the Institutional Animal Care and Use Committee (NO.: INH2018/017), Singapore. The aim was to show the feasibility of using this suturing system in closing an incision endoscopically in a realistic surgical scenario. Porcine models were chosen because of the presence of similar peristalsis, intraluminal secretions, and possible complications in the human colon. Details on the preparation of the animal are provided in Supplementary Material B.

Figure 7 shows the setup. The endoscope was inserted into the pig's rectum. Following submucosal saline lift using an injection needle, a 10 mm submucosal incision was cut in the rectal mucosa using DualKnife. The needle driver and grasper were delivered to the incision site through the two channels of the endoscope. Following the deployment procedure described in [10], the needle with a 10 cm 3-0 Vicryl suture was deployed by tensioning the thin nitinol guidewire. After locking the needle to one jaw of the needle driver and removing the guidewire, four running stitches were made for the incision with the above mentioned "in-out-out-in" pattern. The stitches were secured with a Surgeon's Knot. The knot was created by passing the needle through suture loops, following the procedure illustrated in Figure 4. A monopolar diathermy cutter (Ø2.5 mm) was used to cut the two ends of the suture. The needle was unlocked from the suturing device and subsequently gripped and taken out by the grasper through the tool channel. After withdrawing the needle driver from the endoscope, the endoscope was removed. The animal was euthanized after the procedure.

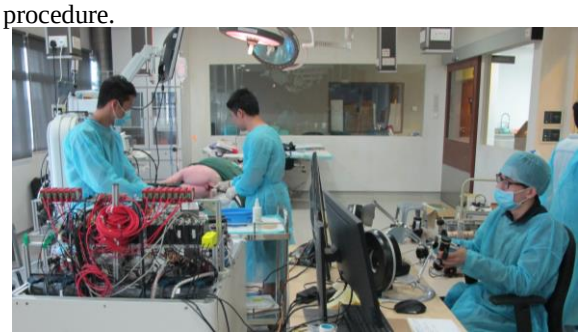

Figure 7. In vivo animal study setup

V. Results and Discussions

A. *Force capabilities of robotic instruments*

As shown in Figure 8, the grasper has a much higher gripping force than the needle driver because the former is shorter in length and has fewer TSMs inside. From C1 to C6, the output force decreases because the mechanical advantage decreases and the joints are in increasingly critical angles in these configurations. However, the gripping forces of the needle driver and the grasper are about 2.5 N and 4.8 N even at the most critical configuration (C3) and they can be 4.3 N and 5.8 N when the arms are straight (C1). These capacities are sufficient for most cases (Section V-B).

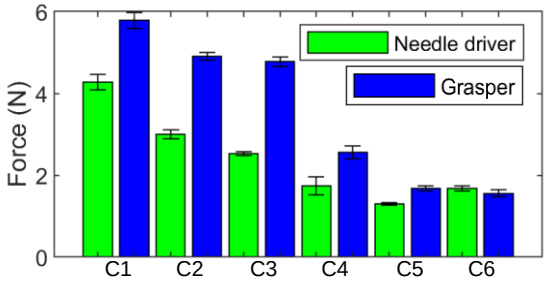

Figure 8. Output force capacities of the robotic needle driver and the grasper at different configurations. C1~C3 are for gripping forces, C4~C5 yaw steering forces, and C6 pitch steering forces. (refer to subsection IV-A for the detailed definitions of C1~C6)

B. *Puncture force of ex-vivo tissues*

As shown in Figure 9a and 9b, when the tendon displacement increases, the upper jaw closes and the force

applied by the needle to the tissue increases; once the tissue is fully penetrated (puncture point), the force suddenly drops. Then, the force rises again as the needle tip reaches the mechanical limit. As the tissue gets ticker, the average puncture force increases (Figure 9c and 9d). The puncture force for stomach tissue is normally higher than that for colon tissue since the former is generally stronger (or tougher) than the latter. The measured puncture forces for colon and stomach tissues are in the range of 0.6 to 3.4 N, which is within the force capability of the needle driver. Note that this is only ex-vivo measurements on pig tissues while more accurate data need to be measured in vivo (ideally, in human bodies) with small force sensors [12, 13] on the needle driver.

The sudden drop of the force at the puncture point always comes with a snapping motion of the upper jaw, which can also be seen through the endoscope camera by the user during suturing. The snapping motion means that the tissue is punctured and the needle quickly reaches the mechanical end and thus is ready to be switched to the opposite jaw. This visual clue is critical for successful needle swapping and has been utilized during the following in vivo study.

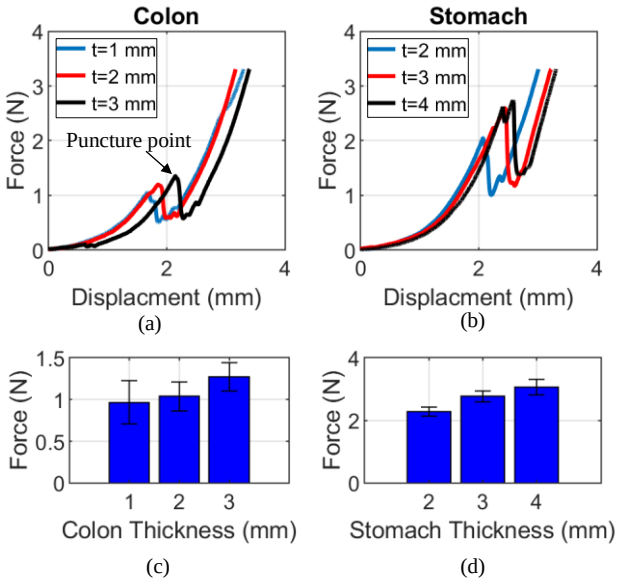

Figure 9. Puncture tests on ex-vivo pig colon and stomach tissues: (a)–(b) force trajectory examples (with respect to tendon displacements) for colon and stomach tissues, respectively; (c)-(d): averages and standard deviations of the puncture forces of colon tissues and stomach tissues, respectively.

C. *In vivo Animal Trials*

The suturing process is shown in Figure 10. The needle driver on the right can accurately point the needle tip to the desired stitching point (Figure 10b) and to the suture loop (Figure 10d). Meanwhile, the grasper on the left played an important role in lifting and feeding tissue to the needle driver as well as handling the suture thread. The time for making the stitches, and creating the knot was 11 mins and 4 mins, respectively. For details, refer to the supplementary video online.

The needle locking mechanism was reliable and ensured successful needle switching during the trial. When the needle penetrated through tissue, the rotating jaw always had a snapping motion (Section V-B) and the needle tip became visible, both of which indicated that the needle was ready to be switched. Apart from the pitch and yaw DOFs, we also found that the rolling DOF was highly important as it helps the end-effectors approach the tissue from a proper angle, which is necessary for incisions with arbitrary orientations. The through-the-scope feature is particularly useful when a new needle needs to be used for additional stitches. The feasibility of deploying the needle using a nitinol guidewire was also confirmed robust. We also confirmed that, as illustrated in Figure 3, puncturing tissue with the needle on the lower jaw is much more efficient than puncturing with the needle on the upper jaw.

With the robotic suturing system, suturing is done by two cooperative robotic instruments, which naturally suits the suturing tasks. This made suturing with this system easier and more intuitive as compared with other devices. In addition, this system supports endoscopic knot-tying (not possible with other devices) and is also compatible with barbed sutures and miniaturized fasteners [14], giving surgeons more choices.

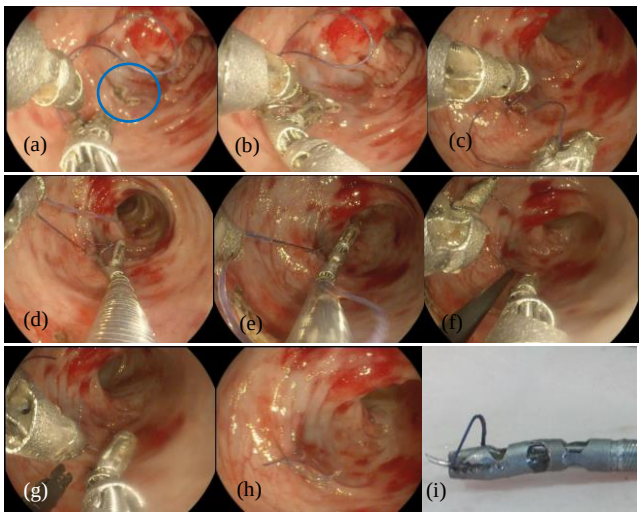

Figure 10. Suturing process. (a) robotic arms deployed at the incision site (highlighted in the blue circle); (b) driving the needle through the tissue; (c) four stitches made; (d) create surgical knot by passing the needle through suture loops; (e) securing the knot by translating the robotic arms into opposite directions; (f) cutting the suture using an electric clutch cutter; (g) withdrawing the needle using the grasper; (h) incision closed using four stitches and a Surgeon's Knot; (i) needle taken out by the grasper.

The current system has some limitations. Suturing in this trial took much longer time than previous ex-vivo trials [10] because of the limitation of the system in sealing insufflation gas. The time can be significantly shortened with proper insufflation. Although the two robotic arms are dexterous in their workspaces, the movement of the endoscope manually controlled by the endoscopist does help. This can be improved via the optimal design of the instruments for larger and more dexterous workspaces. In addition, the camera's view to the needle tip and target suturing point may be blocked by the jaws of the instruments, which sometimes requires the surgeon to adjust the orientation of the instrument for a clear view. This visual occlusion may be avoided using a rotatable or steerable camera with automated algorithms [15]. The current haptic feedback is based on proximal force sensing. Accurate distal force feedback may be enabled using force sensors [16] or modeling [17, 18] to improve stitching and knot-tying. For enhanced safety and efficiency, virtual fixtures [19] may be implemented, and they can be determined in vivo with accurate force feedback during registration. In this trial, gas insufflation was used since the colon was not fully perforated. In the case of perforations, a deployable "tent" [20] may be used to maintain the field of view. The jaws can

only open 78˚ because of unilateral opening while bilateral opening jaws may be developed to enhance the reach of the instruments and to allow suturing for thicker tissues.

VI. Conclusions

This paper presents a novel robotic suturing system to endoscopically suture defects resulted from complex flexible endoscopic procedures with stitches and knots which are not possible with existing endoscopic closure devices. The needle driver ensures efficient and reliable needle manipulation, and the grasper assists by handling tissue and suture threads. Both articulated arms have five DOFs and are intuitively controlled by the surgeon at the master console for dual-arm suturing.

Through the in vivo animal study, this suturing system, with the favorable features listed in Section I, has preliminarily demonstrated its effectiveness of closing gastrointestinal defects endoscopically in realistic surgical scenarios. Since the system enables both stitching and knot-tying, similar to laparoscopic suturing, the closure quality using our suturing method is expected to be similar to surgical closure via laparoscopy. The applications of this technology for perforations in ESD, EFTR, and NOTES are expected.

For future work, the quality of the stitches and knots created using this system will be evaluated; accurate distal force feedback may be displayed to the surgeon for more accurate and efficient suturing; the learning curve of the system will be studied; NOTES procedures using this system will be performed.

Acknowledgments

This research is funded by National Research Foundation (NRF) Singapore (NRF-NRFI2016-07). We also acknowledge equipment support from EndoMaster Pte. Ltd., Singapore.

References

[1] A. Schmidt, B. Meier, and K. Caca, "Endoscopic Full-Thickness Resection: Current Status," *World journal of gastroenterology: WJG*, vol. 21, p. 9273, 2015.

[2] N. de'Angelis, S. Di Saverio, O. Chiara, *et al.*, "2017 Wses Guidelines for the Management of Iatrogenic Colonoscopy Perforation," *World journal of emergency surgery : WJES*, vol. 13, pp. 5-5, 2018.

[3] T. H. Lüning, M. E. Keemers-Gels, W. B. Barendregt, A. C. I. T. L. Tan, and C. Rosman, "Colonoscopic Perforations: A Review of 30,366 Patients," *Surgical Endoscopy*, vol. 21, pp. 994-997, 2007.

[4] A. Arezzo and M. Morino, "Endoscopic Closure of Gastric Access in Perspective Notes: An Update on Techniques and Technologies," *Surgical Endoscopy*, vol. 24, pp. 298-303, 2010.

[5] G. S. Raju, I. Ahmed, G. Shibukawa, A. Poussard, and D. Brining, "Endoluminal Clip Closure of a Circular Full-Thickness Colon Resection in a Porcine Model (with Videos)," *Gastrointestinal Endoscopy*, vol. 65, pp. 503-509, 2007.

[6] G. Iabichino, L. H. Eusebi, M. A. Palamara, *et al.*, "Performance of the over-the-Scope Clip System in the Endoscopic Closure of Iatrogenic Gastrointestinal Perforations and Post-Surgical Leaks and Fistulas," *Minerva Gastroenterologica e Dietologica*, vol. 64, pp. 75-83, 2018.

[7] S. H. Chon, U. Toex, P. S. Plum, *et al.*, "Successful Closure of a Gastropulmonary Fistula after Esophagectomy Using the Apollo Overstitch and Endoscopic Vacuum Therapy," *Endoscopy*, vol. 50, pp. E149-E150, 2018.

[8] S. V. Kantsevoy and J. R. Armengol-Miro, "Endoscopic Suturing, an Essential Enabling Technology for New Notes Interventions," *Gastrointestinal Endoscopy Clinics of North America*, vol. 26, pp. 375-384, 2016.

[9] B. P. M. Yeung and P. W. Y. Chiu, "Application of Robotics in Gastrointestinal Endoscopy: A Review," *World journal of gastroenterology*, vol. 22, pp. 1811-1825, 2016.

[10] L. Cao, X. Li, P. T. Phan, A. M. H. Tiong, J. Liu, and S. J. Phee, "A Novel Robotic Suturing System for Flexible Endoscopic Surgery," in *IEEE International Conference on Robotics and Automation (ICRA)*, Montreal, Canada, 2019, pp. 1524-1520.

[11] L. Rawlins, M. P. Rawlins, and D. Teel, "Human Tissue Thickness Measurements from Excised Sleeve Gastrectomy Specimens," *Surgical Endoscopy*, vol. 28, pp. 811-814, 2014.

[12] W. Lai, L. Cao, Z. Xu, P. T. Phan, P. Shum, and S. J. L. Phee, "Distal End Force Sensing with Optical Fiber Bragg Gratings for Tendon-Sheath Mechanisms in Flexible Endoscopic Robots," in *IEEE International Conference on Robotics and Automation (ICRA)*, Brisbane, Australia, 2018.

[13] W. Lai, L. Cao, R. X. Tan, *et al.*, "An Integrated Sensor-Model Approach for Haptic Feedback of Flexible Endoscopic Robots," *Annals of Biomedical Engineering*, 2019.

[14] C. Y. Lee, C. A. Johnson, J. A. Siordia, J. M. Lehoux, and P. A. Knight, "Comparison of Automated Titanium Fasteners to Hand-Tied Knots in Open Aortic Valve Replacement," *Innovations*, vol. 13, pp. 29-34, 2018.

[15] N. Sarli and N. Simaan, "Minimal Visual Occlusion Redundancy Resolution of Continuum Robots in Confined Spaces," in *2017 IEEE/RSJ International Conference on Intelligent Robots and Systems (IROS)*, 2017, pp. 6448-6454.

[16] W. Lai, L. Cao, R. X. Tan, *et al.*, "Force Sensing with 1mm Fiber Bragg Gratings for Flexible Endoscopic Surgical Robots," *IEEE/ASME Transactions on Mechatronics*, pp. 1-1, 2019.

[17] X. Li, L. Cao, A. M. H. Tiong, P. T. Phan, and S. J. Phee, "Distal-End Force Prediction of Tendon-Sheath Mechanisms for Flexible Endoscopic Surgical Robots Using Deep Learning," *Mechanism and Machine Theory*, vol. 134, pp. 323-337, 2019.

[18] X. Li, A. M. H. Tiong, L. Cao, W. Lai, P. T. Phan, and S. J. Phee, "Deep Learning for Haptic Feedback of Flexible Endoscopic Robot without Prior Knowledge on Sheath Configuration," *International Journal of Mechanical Sciences*, vol. 163, p. 105129, 2019.

[19] L. Wang, Z. Chen, P. Chalasani, *et al.*, "Force-Controlled Exploration for Updating Virtual Fixture Geometry in Model-Mediated Telemanipulation," *Journal of Mechanisms and Robotics*, vol. 9, pp. 021010-021010-11, 2017.

[20] M. Miyasaka, J. J. Liu, L. Cao, and S. J. Phee, "Pneumatically Actuated Deployable Tissue Distension Device for Notes for Colon," in *IEEE International Conference on Robotics and Automation (ICRA)*, Montreal, Canada, 2019.

Supplementary Material A: Motor Blocks

Each DC motor block, with eight DC motors (2657W024CR, Faulhaber Inc, Germany) arranged in a 4×2 array, actuates the respective slave robotic arm through TSMs (Asahi Inc., Japan). In the DC motor block, there is also a load cell (LTH 300, Futek Inc., USA) for each TSM to sense the actuation forces. The compression force on the sheath, which equals the tension force on the tendon, is measured by the corresponding hollow load cell, as shown in Figure S1a. Each articulated joint of the robotic arms is driven by two TSMs and two motors for bi-directional motion control. Each DC motor in the motor block, with a gearhead (gear ratio: 86:1) and a Ø36mm output wheel, can generate 120 N force with a rated speed of 100 mm/s.

Figure S1b shows how the instrument is rolled and translated at the proximal end. The instrument shaft is fixed by a pin vise which rotates with the gears (gear ratio: 2:1)

driven by a DC motor. The DC motor and gears are placed on the moving part of the linear slider (EZ limo, Oriental Motor Co., Japan) which can move the instrument forward and backward. The pin vise allows the instrument to be easily fixed or removed from this driving block and thus facilitates tool exchange. The linear slider can travel 150 mm with a maximum speed of 300mm/s, and the motion resolution is 0.01 mm. The maximum push and thrust forces of the linear slider is 330 N and 157 N, respectively.

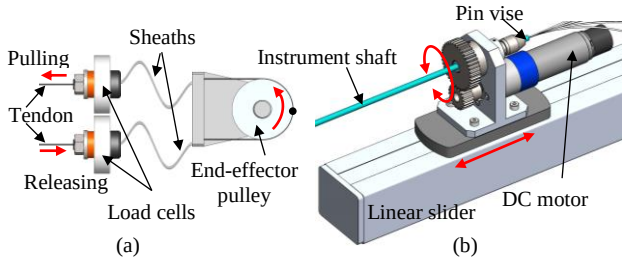

Figure S1. (a) Actuation and force sensing principle for TSM; (b) actuation module for roll and translation DOFs.

Supplementary Material B: Preparation of the Animal

For four days prior to the procedure, the animal had been fed a liquid diet and 1 sachet of Fortrans ® (PEG-Electrolyte Powder) in 1 liter of solution was administered twice a day to the animal to clear the intestines of any solid food. Bowel preparation was monitored closely to ensure that the colon was clear of any solid wastes. One day before the procedure, the animal was placed on a honey water diet. Fleet enema was administered to ensure that the colon was properly cleared and purged and the animal was expelling only clear or light brownish fluid. On the day of the procedure, the animal was pre-medicated using Atropine Sulphate (50ug/kg, IM). The animal was under general anesthesia during the procedure.